

The Cause of the Superoutburst in SU UMa Stars is Finally Revealed by Kepler Light Curve of V1504 Cygni

Yoji OSAKI

Department of Astronomy, School of Science, University of Tokyo, Hongo, Tokyo 113-0033
osaki@ruby.ocn.ne.jp

and

Taichi KATO

Department of Astronomy, Kyoto University, Sakyo-ku, Kyoto 606-8502
tkato@kusastro.kyoto-u.ac.jp

(Received 201 0; accepted 201 0)

Abstract

We have studied the SC (short cadence) Kepler light curve of an SU UMa star, V1504 Cyg, which extends for a period of about 630 d. All superoutbursts in V1504 Cyg have turned out to be of the precursor-main type and the superhump first appears near the maximum of the precursor. The superhumps grow smoothly from the precursor to the main superoutburst showing that the superoutburst is initiated by the tidal instability (as evidenced by growing superhump) as envisioned in the thermal-tidal instability (TTI) model proposed by Osaki (1989). We have performed power spectral analysis of the light curve of V1504 Cyg. One of outstanding features is an appearance of a negative superhump extending for around 300 d, well over a supercycle. We have found that an appearance of the negative superhump tends to reduce the frequency of occurrence of normal outbursts. Two types of supercycles are recognized in V1504 Cyg, which are similar to those of the Type L and S supercycles in the light curve of VW Hyi, a prototype SU UMa star, introduced by Smak (1985). It is found that the Type L supercycle is the one accompanied with the negative superhump and the Type S is that without the negative superhump. If we adopt a tilted disk as an origin of the negative superhump, two types of the supercycles are understood to be due to a difference in outburst intervals, which is in turn caused by a difference in mass supply from the secondary to different parts of the disk. The frequency of the negative superhump varies systematically during a supercycle in V1504 Cyg. This variation can be used as an indicator of the disk radius variation and we have found that observed disk radius variation in V1504 Cyg fits very well with a prediction of the TTI model.

Key words: accretion, accretion disks — stars: dwarf novae — stars: individual (V1504 Cyg) — stars: novae, cataclysmic variables

1. Introduction

The SU UMa stars are dwarf novae in short orbital periods which show two distinct types of outbursts: short normal outburst with a duration of a few days and long superoutburst with a duration of typically two weeks [see, Warner (1995) and Hellier (2001a) for dwarf novae in general and SU UMa stars in particular]. In ordinary SU UMa stars, several short normal outbursts are sandwiched by two long superoutbursts and a cycle from one superoutburst to the next is called the supercycle. The normal outbursts are believed to be essentially the same as those outbursts observed in ordinary dwarf novae with longer orbital periods such as U Gem or SS Cyg stars and they are now well understood by the thermal limit-cycle instability in the accretion disk (e.g., see Cannizzo 1993, Lasota 2001). During the superoutburst, periodic humps called the superhumps always appear with a period slightly longer than the orbital period by a few percent. The superhump phenomenon is now well understood by the tidal instability (Whitehurst 1988, Hirose, Osaki 1990,

Lubow 1991): superhumps are produced by the periodic tidal stressing of the eccentric precessing accretion disk, which is in turn produced by the tidal 3:1 resonance instability between accretion disk flow and orbiting secondary star.

As for the superoutbursts and supercycles in SU UMa stars are concerned, three different models have so far been proposed; the thermal-tidal instability model advocated by Osaki, the enhanced mass-transfer model advocated by Smak, and the pure thermal instability model by Cannizzo. No consensus has yet been reached about the cause of the superoutburst.

Besides the original planet hunting mission, NASA's Kepler observations (Koch et al. 2010) with high accuracy photometry give an unprecedented opportunity to investigate variable stars. Two SU UMa stars, V344 Lyr and V1504 Cyg, in the Kepler field have been observed with the short cadence (SC) mode and some of their light curves are now available to public. In this paper, we study the cause of the superoutburst in SU UMa stars by using the Kepler light curve of one of SU UMa stars, V1504 Cyg,

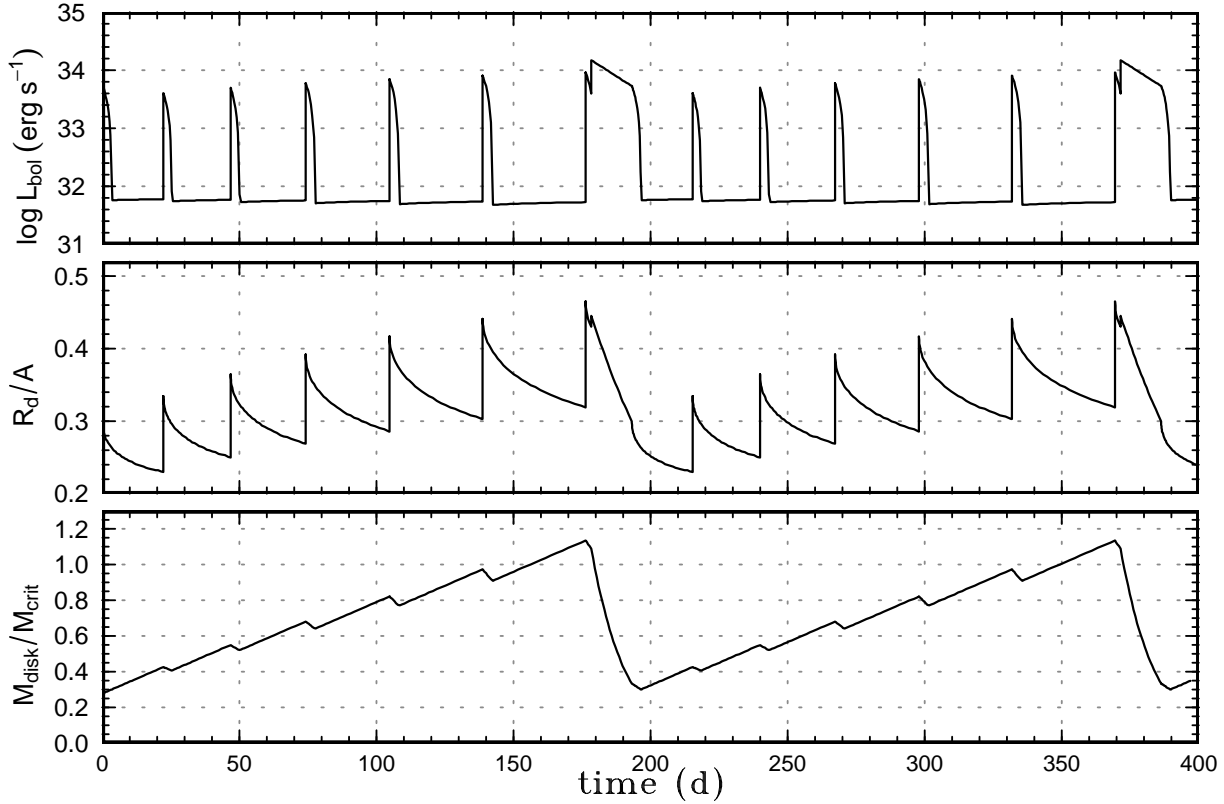


Fig. 1. Time evolution of an accretion disk in a supercycle based on the simplified form of the TTI model, redrawn using the result in Osaki (2005). Two supercycles are shown in the figure for clarity. The model parameters used are those of VW Hyi, a prototype SU UMa star. From the top to the bottom, (upper:) bolometric light curve, (middle:) the disk radius variation in units of the binary separation A , (lower:) the total disk mass M_{disk} normalized by the critical mass M_{crit} above which the disk can be tidally unstable.

in section 3.

Before going into the study of Kepler data, we review three models for superoutbursts and supercycles of SU UMa stars in section 2. For convenience, we summarize in table 1 the main difference between three models and what we regard as consequences of these models to be compared with observation.

2. Superoutburst Models

2.1. Thermal-tidal Instability Model (TTI model)

As for the superoutburst and supercycle of SU UMa stars, Osaki (1989) proposed a model (now called the thermal-tidal instability model, or TTI model in short) in which the ordinary thermal instability is coupled with the tidal instability [see, Osaki (1996) for a review]. The TTI model is basically the disk instability variety in which the mass-transfer rate from the secondary is assumed to be constant and all variability is thought to be produced within the disk.

The TTI model explains the supercycle of SU UMa stars in the following way. In the initial stage of the supercycle, the disk is assumed to be compact well below the 3:1 resonance radius. A successive outburst (normal outburst) causes mass accretion onto the central white dwarf but the accreted mass is less than mass transferred during quies-

cence. The mass and angular momentum of the disk are accumulated and disk's outer edge therefore grows with a succession of normal outbursts and a final normal outburst (a triggering normal outburst) brings disk's outer edge beyond the 3:1 resonance radius $R_{3:1}$ (where $R_{3:1} \simeq 0.46A$ and A is the binary separation). The disk then becomes tidally unstable and a circular disk is transformed to a slowly precessing eccentric disk. The tidal dissipation of the eccentric disk now enhances the mass flow in the disk, sustaining the disk in a hot state for a longer superoutburst. When sufficient mass is drained from the disk, matter in the outer edge reaches the critical surface density below which no hot state exists. The disk makes a downward transition to a cool state. The cooling front propagates inward, extinguishing the outburst, i.e., an end of superoutburst. The eccentric disk eventually returns back to a circular disk because of addition of matter of low specific angular momentum. Because of the enhanced tidal torque during the superoutburst stage, the disk becomes compact in the end. A new supercycle begins. This is the basic picture of the TTI model but minor modification and further refinement to this model have been proposed by Hellier (2001b) and by Osaki, Meyer (2003) and by Osaki (2005).

Osaki (1989) have calculated light curves of SU UMa stars by using a simplified semi-analytic model, a model

Table 1. Comparison of models for superoutbursts and superhumps.

Models				
	thermal-tidal (TTI)	instability	enhanced (EMT)	mass-transfer pure thermal instability
major advocator	Osaki		Smak	Cannizzo
mass-transfer rate from the secondary (\dot{M}_{tr})	constant		variable	constant
origin of superhump	eccentric disk		variable hot spot brightness	(eccentric disk?)
origin of superoutburst	enhanced tidal torque		enhanced mass-transfer	wide outburst
main point of the model	disk radius variation in su- percycle		EMT due to irradiation of the secondary	pure thermal instability is complex enough to produce superoutburst and supercycle
major premises of the model	(1) constant \dot{M}_{tr}		(1) enhanced mass transfer from the secondary due to irradiation heating	(1) pure thermal instability
	(2) tidal instability and ec- centric disk responsible for superhump and superout- burst		(2) variable and enhanced hot spot during superout- burst	(2) superhump is of sec- ondary importance (3) normal outbursts are “inside-out”

Major consequences discussed in this paper[†]

expansion of the disk during normal outburst	Yes		Yes	<u>No</u>
outside-in type normal outburst	Yes		NA*	<u>No</u>
humps during the last normal outburst before superoutburst	failed superhumps		<u>enhanced hot spot</u>	NA
distinct precursor out- burst	Yes		Yes	<u>No</u>
appearance of super- hump	peak of precursor		<u>after peak of superoutburst</u>	NA
enhanced hot spot dur- ing superoutburst	No		<u>Yes</u>	No

[†]Underlined items are not in agreement with observation or items need to be explained by the model (see text for details).

*Not applicable.

consisting of a torus plus an inviscid disk having power-law surface-density distribution. Figure 1 illustrates one of such light curves together with the disk radius variation and the disk mass variation. Here we note that all outbursts in this model is of “outside-in” (here “outside-in” means an outburst in which transition to hot state first occurs at the outer part of the disk and the heating wave propagates inward while “inside-out” does that in which transition to hot state occurs at the inner part and the heating wave propagates outward).

As far as mass accumulated during a supercycle is concerned, the difference between a normal outburst just prior to a superoutburst and the next superoutburst is rather small as seen in the lowest panel of figure 1. However, there is a big difference between these two states concerning about tidal removal of angular momentum from the disk. In the case of a normal outburst, the disk’s outer edge is below the tidal 3:1 resonance radius and thus the tidal removal of angular momentum is very ineffective. On the other hand, the disk’s outer edge exceeds the tidal 3:1 resonance radius in the last normal outburst or the triggering outburst (which is a part of precursor of a superoutburst). The tidal instability then develops, which is observationally seen as growing superhumps. As discussed in Osaki, Meyer (2003) and Osaki (2005), in the case of no effective tidal removal of angular momentum from the disk, an expansion of the disk due to the thermal instability immediately brings back the surface density at the outer edge of the disk to the critical density below which there exists no hot state. The disk then makes downward transition to the cool state and the cooling wave propagates inward and the outburst is short. This is the reason why a normal outburst just prior to a superoutburst is so short even if mass is sufficiently accumulated in the disk.

The key point of the TTI model lies in the disk radius variation shown in the middle panel of figure 1. This has to be tested observationally but it has been difficult before the Kepler observations.

Ichikawa et al. (1993) have performed light curve simulations of superoutburst and supercycle of SU UMa stars by using one-dimensional numerical code based on the TTI model. Two different prescriptions for the viscosity in the cold state (i.e., α_{cold}) have been examined there. One is for the case of outside-in normal outbursts in which the α viscosity has a radial dependence (called there “case A”) and the other is for the case of inside-out normal outbursts (“case B”) in which the α viscosity is constant with respect to radius. It has been shown that the quiescent intervals between normal outbursts increase monotonically with the advance of supercycle phase in the case A (see, their figure 1) while they stay almost constant during a supercycle in the case B (see, their figure 2). This point will be discussed later with Kepler light curves. Buat-Ménard, Hameury (2002) have performed light curve simulations by using their code, confirming that the TTI model can account for the SU UMa light curves. Two dimensional smoothed particle hydrodynamics (SPH) code simulations of superhumps and superoutbursts of SU UMa stars were performed by Murray (1998) and Truss et al. (2001), confirm-

ing that the superoutburst and superhump phenomenon is a direct result of the tidal instability. Smith et al. (2007) made 3D SPH simulations of superhumps and found enhanced tidal torques to transfer the angular momentum from the disk to the binary orbital motion when the eccentric instability develops, as suggested in the TTI model.

Two alternative models to explain the superoutburst phenomenon have been proposed besides the TTI model. One of them is the enhanced mass-transfer model (EMT model) due to irradiation heating of the secondary star, advocated by Smak. The other is the pure thermal instability model by Cannizzo et al. (2010).

2.2. The Enhanced Mass-Transfer Model (EMT model)

The enhanced mass-transfer model for superoutbursts of SU UMa stars was first proposed by Vogt (1983), and discussed by Osaki (1985). In this model, the superoutburst of SU UMa stars is produced by enhanced mass transfer from the secondary star, which is in turn caused by irradiation heating of the secondary star. Osaki (1985) proposed an EMT model, a model of the irradiation-induced mass-overflow instability as a possible cause of superoutbursts in SU UMa stars. However, Osaki (1996) abandoned this model later in favor of the TTI model. Smak pursued this model instead.

Smak (1991), Smak (2004), Smak (2008) has been writing a series of papers in *Acta Astronomica* in which he criticizes the TTI model and instead he advocates the enhanced mass-transfer (EMT) model. In the EMT model, the long duration of the superoutburst of SU UMa stars is thought to be produced by enhanced mass transfer from the secondary star, which is in turn caused by the irradiation heating of the atmosphere of the secondary star due to ultraviolet radiation from the mass accreting white dwarf and the boundary layer between the accretion disk and the central white dwarf. In the EMT model the superhump phenomenon is not directly related with the mechanism of superoutburst. Rather the superhump is thought to be produced by modulated dissipation of gas stream due to modulated mass outflow which is in turn produced by periodically variable irradiation of the secondary star (Smak 2009).

As Smak (1991), Smak (1996), Smak (2000) clearly stated, he was motivated to pursue the EMT model because of following two seeming difficulties in the TTI model, to which we address in this paper.

1. Observational evidence for enhanced mass transfer: Vogt (1983) argued in his review on VW Hyi that the amplitude of the orbital humps is increased in maximum or decline stage of normal outbursts if they occur less than 40 d before the next superoutburst, and interpreted that the mass-transfer rate from the secondary star is enhanced. Smak (1991) regarded this point as one of difficulties of TTI model.
2. Sequence of events which TTI model predicts: Smak raised another question to TTI model which is connected with the sequence of events responsible for superoutbursts and superhumps. He argued

that in the TTI model it begins with a tidal instability, leading to the formation of an eccentric disk, and causing a major enhancement of the accretion rate. Accordingly the superhump should appear at the very early phase of a superoutburst (certainly not later than maximum). In most cases, however, they appear one or two days *after the superoutburst maximum*.

Regarding the point 1, Osaki, Meyer (2003) already questioned Vogt's interpretation of "orbital humps" and suspected that the observed humps could be of superhump nature. This is the very controversy about the nature of observed humps. These two problems raised by Smak will be discussed with the Kepler light curve of V1504 Cyg.

Light curve simulations based on the EMT model was made by Smak (1991), and Schreiber et al. (2004). Schreiber et al. (2004) have performed light curve simulations both in the TTI model and EMT model and they compared their results with multi-wavelength light curves of VW Hyi, one of the best observed SU UMa stars before the Kepler observations. All outbursts in their models have turned out to be of inside-out type because of their viscosity prescription. It has been found there that both models can generate precursor outbursts which are more pronounced at shorter wavelengths, in agreement with observations. Since there are adjustable free parameters in the numerical light-curve simulations for both the TTI model and the EMT model, Schreiber et al. (2004) stated that it is difficult to decide which models are better in explaining observations. However these authors have concluded that the EMT model is to be favored over the TTI model because the EMT model is more sensitive to mass-transfer rate variation, which is supposed by these authors to be responsible for variations seen in different supercycles in one star and in different SU UMa stars.

In the EMT model mass-transfer rate is thought to be greatly increased during a superoutburst. The response of the secondary's envelope to enhanced mass transfer has to be considered. That is, the response of mass reservoir of envelope of the secondary will affect the recurrence time of supercycle in SU UMa stars. This effect has not been taken into account in simulations of Schreiber et al. (2004) and their results are thus incomplete in this respect.

2.3. The Pure Thermal Limit Cycle Model

Let us now turn to another alternative model of the pure thermal instability model proposed by Cannizzo et al. (2010), Cannizzo et al. (2012) and references therein. In this model, the short normal outburst and the long superoutburst of SU UMa stars are thought to be "narrow" and "wide" outbursts seen in SS Cyg-type dwarf novae of longer orbital period systems, an idea first proposed by van Paradijs (1983). In this model, not only the short normal outburst but also the long superoutburst are explained by the standard thermal limit cycle instability and the tidal instability is not needed to explain the long duration of superoutburst and the supercycle phenomenon in SU UMa stars. The superhump is only an

additional phenomenon and it is of secondary importance. Cannizzo et al. (2010) have performed numerical simulations, demonstrating that the thermal limit cycle instability without tidal instability is complex enough to produce the superoutburst and supercycle of SU UMa stars in which several short outbursts are sandwiched by two long outbursts.

In Cannizzo's pure thermal limit cycle model, the short normal outburst is explained by an inside-out outburst in which an outburst is started in the inner part of the accretion disk and the heating front propagates outward but it does not reach the disk's outer edge but it is reflected in the middle of the disk as a cooling wave [see, figures 3 and 4 of Cannizzo et al. (2010)]. This type of outburst is called as "Type Bb" in Smak's classification and it is known that the disk's outer edge does not expand in this type of outburst even when an outburst occurs (see Smak 1984). In this model, mass in the outer part of the disk is untapped during short normal outbursts but only mass in the inner part is accreted during short normal outbursts. The triggering outburst in this model is also the inside-out outburst but this time the heating front traveling outward finally reaches the disk's outer edge, producing the long superoutburst with the viscous plateau stage (i.e., Smak's Type Ba outburst).

As discussed by Smak (1984), alternation of narrow and wide outbursts can be produced in the case of the inside-out outbursts. On the other hand, in the case of the outside-in outbursts, widths of outbursts are more or less similar. If any normal outburst in SU UMa stars turns out to be outside-in by observations, Cannizzo's model will meet a serious difficulty. We shall discuss below Cannizzo's pure thermal instability model as well.

3. Kepler Light Curve of V1504 Cyg

Kepler observations now open a possibility to discriminate between these three models of SU UMa stars from the purely observational point of view. Two SU UMa type dwarf novae, V1504 Cyg and V344 Lyr, were observed with the short cadence (SC) mode by the Kepler satellite. These light curves have already been studied by Cannizzo and his group, i.e., about quiescent superhumps (Still et al. 2010), numerical models of the long term light curve of V344 Lyr (Cannizzo et al. 2010), studies of both positive and negative superhumps in the long term light curve of V344 Lyr (Wood et al. 2011) and a study of the outburst properties of V1504 Cyg and V344 Lyr (Cannizzo et al. 2012). In this paper we examine the same Kepler data of V1504 Cyg but from a different point of view. Data which we have used in this paper extend from 2009 June to 2011 March. We discuss below three problems: about the global light curve in section 3.1 and about how superoutbursts are started in section 3.2, and about the negative superhump in sections 3.3 and 3.4. As seen below, we reach a conclusion quite different from Cannizzo et al. (2012) about the nature of the superoutburst and supercycle.

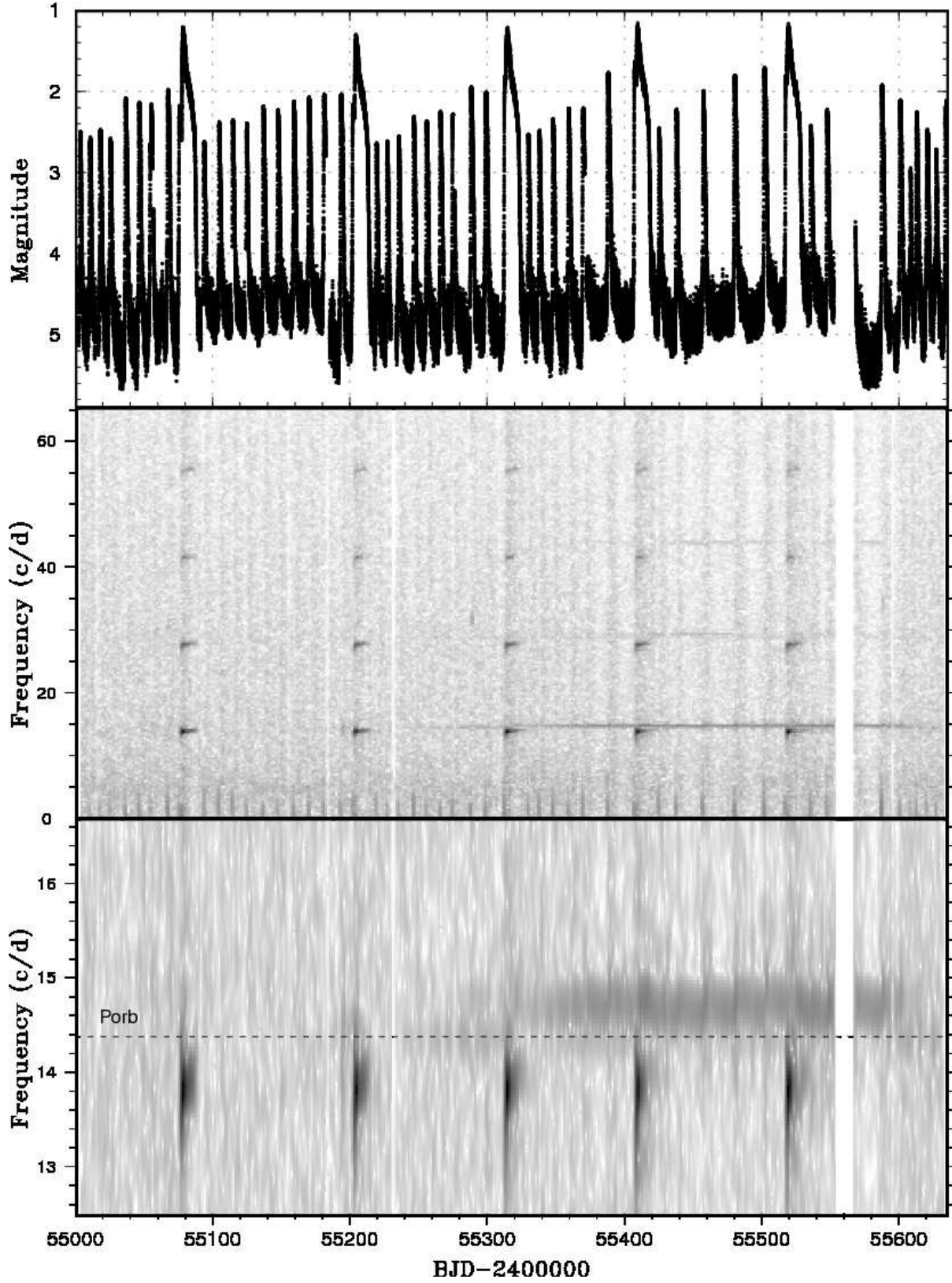


Fig. 2. Two-dimensional power spectrum of the Kepler light curve of V1504 Cyg for the all data. From the top to the bottom, (upper:) light curve; the Kepler data were binned to 0.005 d, (middle:) power spectrum, (lower:) its enlargement for the frequency region around the orbital one. The width of the moving window and the time step used are 5 d and 0.5 d, respectively.

Table 2. Superoutbursts and supercycles of V1504 Cyg.*

(1) SC number	(2) start of SC [†]	(3) start of SO [†]	(4) end of SO [†]	(5) SC length excluding SO [‡]	(6) SO duration [‡]	(7) SC length [‡]	(8) number of NO	(9) negative SH	(10) orbital hump
1	—	74.5	88.5	—	14	>88	>8	no	no
2	88.5	201	215	112.5	14	126.5	10	no	no
3	215	312	325	97	13	110	10	later half	partly
4	325	406.5	419	81.5	12.5	94	6	full	no
5	419	516	530	97	14	111	5	full	no
6	530	—	—	—	—	—	—	early part	later part

*Abbreviations in this table: supercycle (SC), superoutburst (SO), normal outburst (NO), superhump (SH).

[†]BJD–2455000.

[‡]Unit: d.

3.1. Global Light Curves and Supercycles of V1504 Cyg

The Kepler light curves of V1504 Cyg and V344 Lyr, extending 736 d at 1 min cadence have been examined by Cannizzo et al. (2012) and they have studied various correlations, such as quiescence intervals between normal outbursts within a supercycle. Here we examine the same data set of V1504 Cyg from different standpoints. The data we have used are those of public release of 632 d at 1 min cadence. Since Wood et al. (2011) have examined V344 Lyr, we examine here data of V1504 Cyg.

The Kepler light curve of V1504 Cyg was already studied by Kato et al. (2012). We summarize the basic data of V1504 Cyg obtained there: its orbital period is 0.069549 d (1.67 hr or 14.38 c/d), the (ordinary or positive) superhump period is about 0.072 d (13.8 c/d) and the negative superhump period is about 0.067 d. (14.7 c/d).

We have made two-dimensional power spectral analysis (the dynamic spectrum) of light curve of V1504 Cyg and we show our results together with the light curve in figure 2. We used the Kepler raw data (SAP_FLUX) for 632 d from Barycentric Julian Date (BJD) 2455002 to 2455635. In calculating power spectra, we used a locally-weighted polynomial regression (LOWESS: Cleveland 1979) to Kepler magnitudes (on an arbitrary zero-point) in removing trends resulting from outbursts using smoothing parameters ($f=0.0003$, $\delta=0.2$) in R software¹. We then estimated the pulsed flux by multiplying residual amplitudes and LOWESS-smoothed light curve converted to the flux scale. In calculating Fourier spectrum, we used a Hann window function with a 5 d width of moving window, and 0.5 d as time step. Figure 2 shows the overall light curve in the top panel, power spectra in wider frequency range in the middle panel, and their enlarged portion near the orbital frequency of the star, as we are interested in this region.

Let us first look at figure 2 for light curve of V1504 Cyg. The Kepler data of V1504 Cyg we use here contain five superoutbursts and four supercycles and we summarize their main characteristics in table 2. Here we define the start of a supercycle is the start of quiescence just after the

preceding superoutburst and its end is the end of the superoutburst. The first column of table 2 is the supercycle ordinal number of our data while the next three columns give BJD of the start of a supercycle (2), the start of a superoutburst (3), and the end of the superoutburst (4), respectively, counted from BJD 2455000. Thus the date of a start of a supercycle is the same as that of the end of the preceding supercycle, as seen in the table. The following three columns give the lengths in days of a supercycle excluding superoutburst (5), of superoutburst duration (6), and of full supercycle (7), respectively, and thus the sum of the two columns (5) and (6) is equal to the column (7). The next column (8) gives number of normal outbursts within a supercycle. The last two columns (9) and (10) give comments about an appearance (or visibility) of negative superhumps and orbital humps in the power spectrum of figure 2, respectively, where “no” means no strong signals in the power spectrum. We have four complete supercycles No. 2–5, while supercycles No. 1 and No. 6 are incomplete because either the preceding or the following superoutburst is lacking in our data.

As seen in the light curve of figure 2 and in table 2, the most outstanding feature of supercycles in V1504 Cyg is that the number of normal outbursts within a supercycle differs greatly from one supercycle to another, i.e., its number varies from 5 (for supercycle No. 5) to 10 (for supercycles No. 2 and 3) in the case of V1504 Cyg. Although the length of supercycle varies between different supercycles (its average value is about 110 d in V1504 Cyg), their difference is small as compared with the difference in number of outbursts within different supercycles. The duration of superoutbursts is not much different between different supercycles either. This point will be discussed later in this subsection.

Let us now examine the power spectra shown in the middle panel and the lowest panel of figure 2 and also those of individual supercycles in figure 3 for more details where a frequency 14.38 c/d for the orbital period is indicated by dashed line. We see that the strongest signals in the power spectrum occur at frequency around 13.8 c/d, corresponding to that of ordinary (positive) superhumps whenever a superoutburst occurs, a well known fact for SU UMa stars. Its higher harmonics are all visible in

¹ The R Foundation for Statistical Computing:
<http://cran.r-project.org/>.

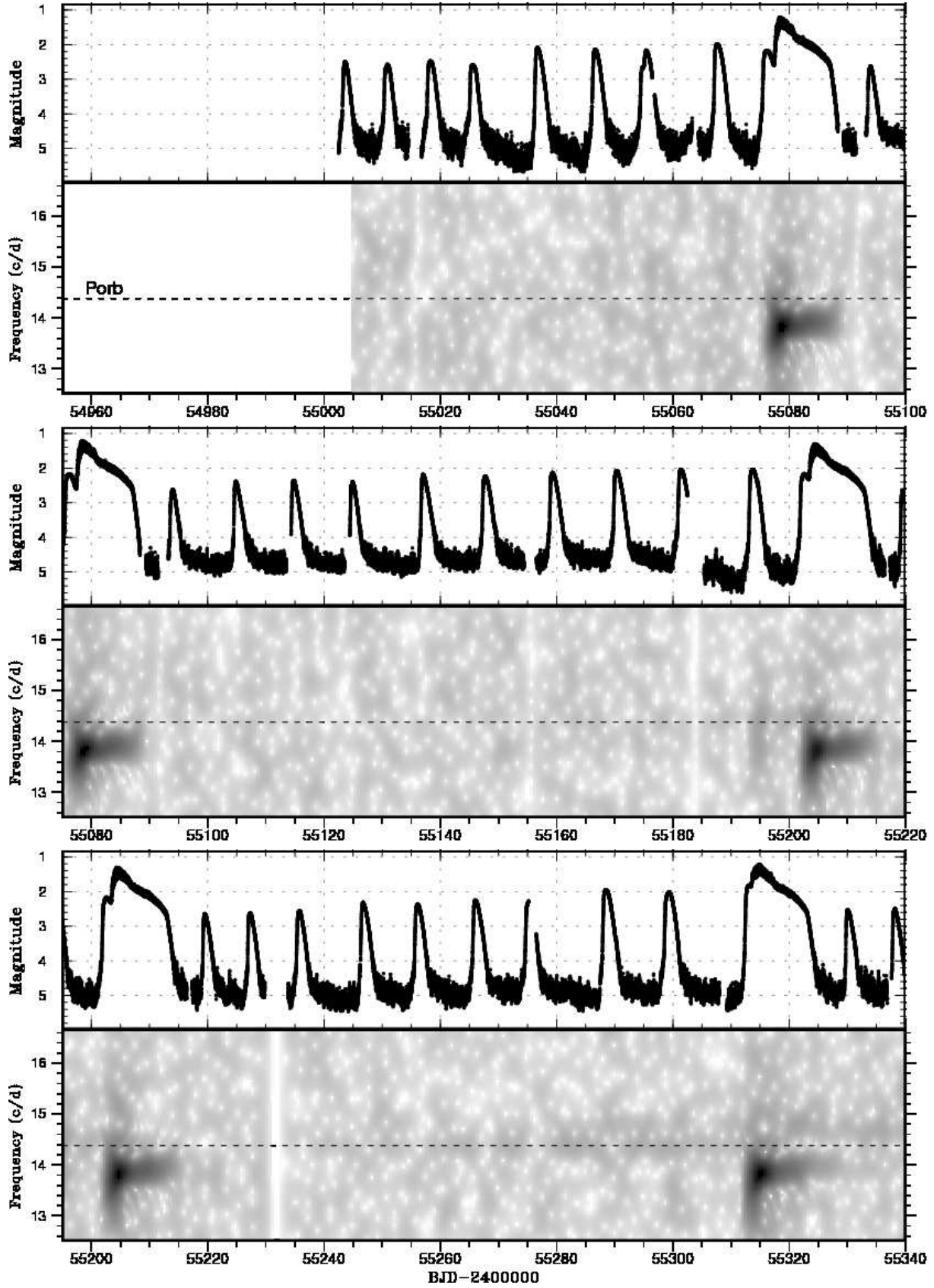


Fig. 3. The same as figure 2 but for six supercycles showing some of detailed features. The upper panel of each supercycle shows the light curve and the lower panel does the power spectrum around the orbital frequency region. The horizontal dash line represents the orbital frequency.

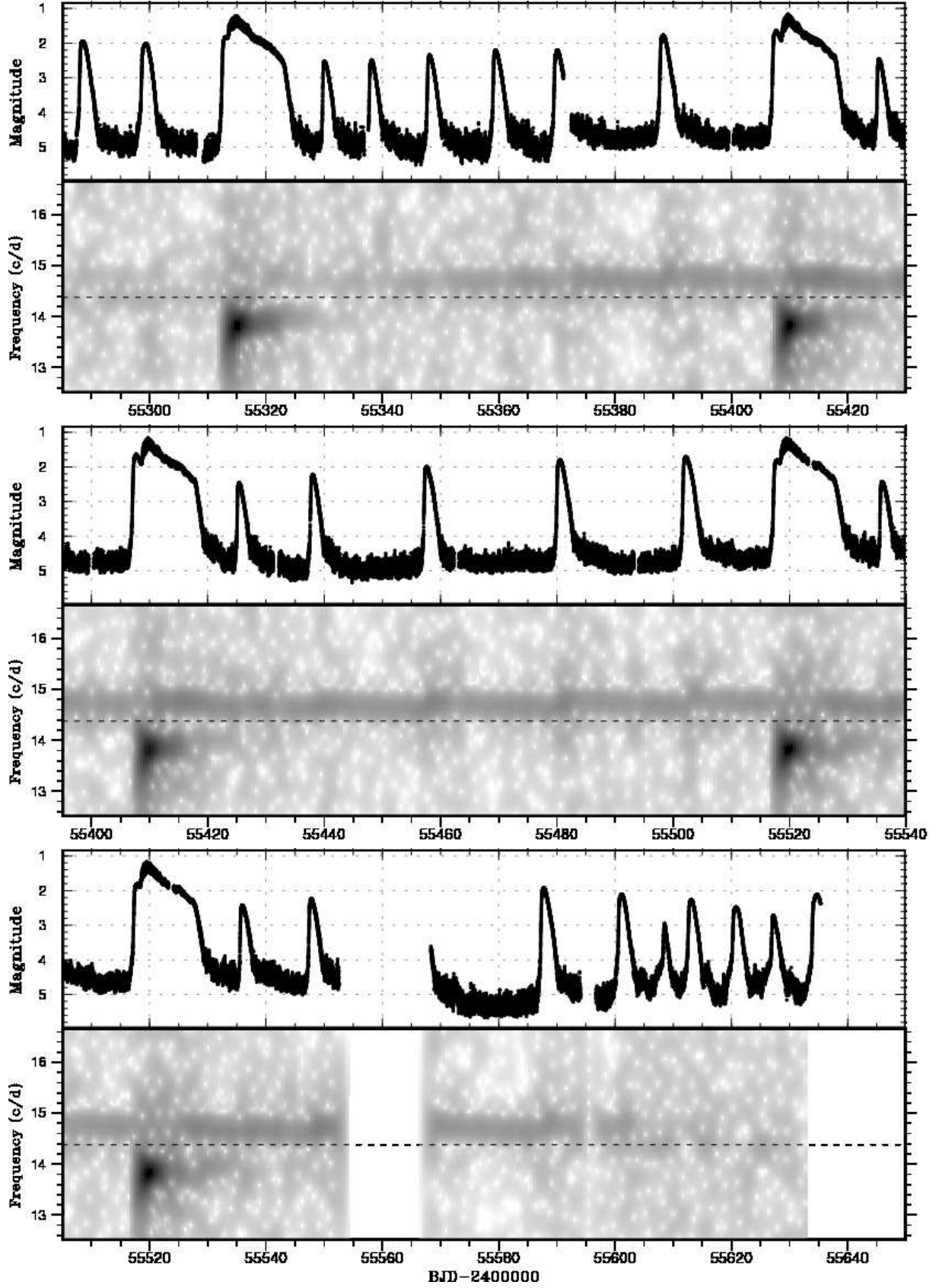


Fig. 3. (continued)

the middle panel of figure 2, indicating the non-sinusoidal waveform of the positive superhump light variation.

The most interesting aspect in the dynamic spectrum is the appearance of a so-called negative hump at frequency around 14.7 c/d. These are humps with a period shorter than the binary orbital period (a few percent shorter than the orbital period). Although the origin of negative superhumps has not been yet firmly established, the standard interpretation is that of retrograde nodal precession of a tilted disk (e.g., Harvey et al. 1995, Montgomery, Martin 2010, Wood et al. 2011). Since there is no viable alternative model, we adopt the model of tilted disk as a working hypothesis and we examine the Kepler data based on this model. In this picture the negative superhumps are produced when the accretion disk is tilted from the binary orbital plane and its nodal line precesses retrograde and the negative superhump periodicity is produced by the synodic period between the retrograde precessing disk and the orbiting secondary star. Light variation with the negative superhump period is thought to be produced by periodic change in dissipation of kinetic energy of gas stream from the secondary star with varying depth of potential well in the disk as it sweeps around the tilted disk (see Wood et al. 2011). When the accretion disk is coplanar with the orbital plane, the gas stream collides with the disk at its outer rim and this produces so-called orbital humps with the binary orbital period.

Negative superhumps for the Kepler data of V344 Lyr have been already discussed from the standpoint of a tilted disk by Wood et al. (2011). In V344 Lyr negative superhumps appeared in quiescence and in normal outbursts and in the other occasion the signature of negative superhump disappeared. A signature of the orbital humps appeared from time to time but these two signals did not seem to exist simultaneously. We see in the lowest panel of figure 2 that the signal of negative superhump appeared in the middle of the supercycle No. 3 in V1504 Cyg. It is not clear when this signal first appeared but a very weak signal is recognized around BJD 2455250. Its intensity increased with time and it is very clearly visible after BJD 2455350 in the later half of the supercycle No. 4. It continued to be seen until BJD 2455600 and it then tapered off.

Most interestingly, the appearance of negative superhumps is strongly correlated with the length of the quiescence interval of outbursts, that is, the quiescence interval between two outbursts becomes longer when the negative superhump appears. That is, the appearance of negative superhumps tends to reduce the frequency of normal outbursts. The same type of phenomena has already been observed in other SU UMa stars with high mass-transfer rates, such as V503 Cyg (Kato et al. 2002, Kato et al. 2013) and ER UMa (Ohshima et al. 2012). Cannizzo et al. (2012) also noticed this in the Kepler light curve of V344 Lyr. In our Kepler data we basically confirm the finding of Kato et al. (2002), Kato et al. (2013) and Ohshima et al. (2012) that the existence of negative superhump suppresses frequent occurrence of normal outbursts.

A similar type of difference in supercycles has been al-

ready noticed in light curves of VW Hyi (a prototype SU UMa star), and Smak (1985) has classified them into two types: Type L supercycle in which the interval of the last two normal outbursts is longer than 30 d and Type S in which it is shorter than 23 d, where the average supercycle length of VW Hyi is about 180 d. The number of normal outbursts in Type L supercycle is small while in Type S it is roughly twice as large as that of Type L. In Type L supercycle of VW Hyi, the quiescence interval between normal outbursts increases monotonically with the advance of supercycle phase while in Type S it increases to the middle of supercycle but it decreases in later half within a supercycle. Smak (1985) has not found any correlation of these two supercycle types with either preceding or following superoutbursts and with any other supercycle properties. Thus the origin of these two types has remained to be a mystery.

Here we make the use of Smak's symbol of Type L and Type S supercycles to our case of V1504 Cyg. We define here that the Type L supercycle is that in which the quiescence interval between two normal outbursts is relatively "long" but the number of normal outbursts within a given supercycle is small, while the Type S is that in which the quiescence interval between two normal outbursts is "short" but the number of normal outbursts within a supercycle is large. However we note that Smak's distinction for Types of L and S in VW Hyi concerns only the last two normal cycles while it applies to most of normal outburst intervals in our case. From figure 2 we find that in V1504 Cyg, supercycles No. 4 and No. 5 correspond to Type L while a supercycle No. 2 corresponds to Type S.

Phenomenologically speaking, we may understand from the Kepler data that the Type L supercycle is a supercycle accompanied with negative superhumps while the Type S supercycle does not have negative superhumps. Furthermore if we adopt a tilted disk as the origin of the negative superhump, we can understand how the two distinct types of supercycle, Type L and Type S, are produced as discussed below.

V1504 Cyg belongs to SU UMa stars with high mass-transfer rates as their supercycle lengths are short (i.e., its mean value of around 110 d), showing frequent normal outbursts. Most normal outbursts in V1504 Cyg are expected to be of outside-in type, which is confirmed by the observed shape of the outburst light curve, i.e., rapid rise to outburst maximum and slow decline from maximum [see, Smak (1984); he calls such an outburst as "type A outburst"]. Cannizzo et al. (2012) also mentioned the same view.

If the disk is co-planar with the binary orbital plane, the gas stream leaving from the inner Lagrangian point of the secondary arrives at the outer rim of the disk. On the other hand, if the disk is tilted, the gas stream sweeps over the tilted disk and it hits the outer rim twice in a synodic period between the retrograde precessing tilted disk and the orbiting secondary star (i.e., the negative superhump period) and in other time it reaches the inner part of the disk. In such a case matter arriving at the outer edge is effectively reduced, even if mass-transfer rate from the

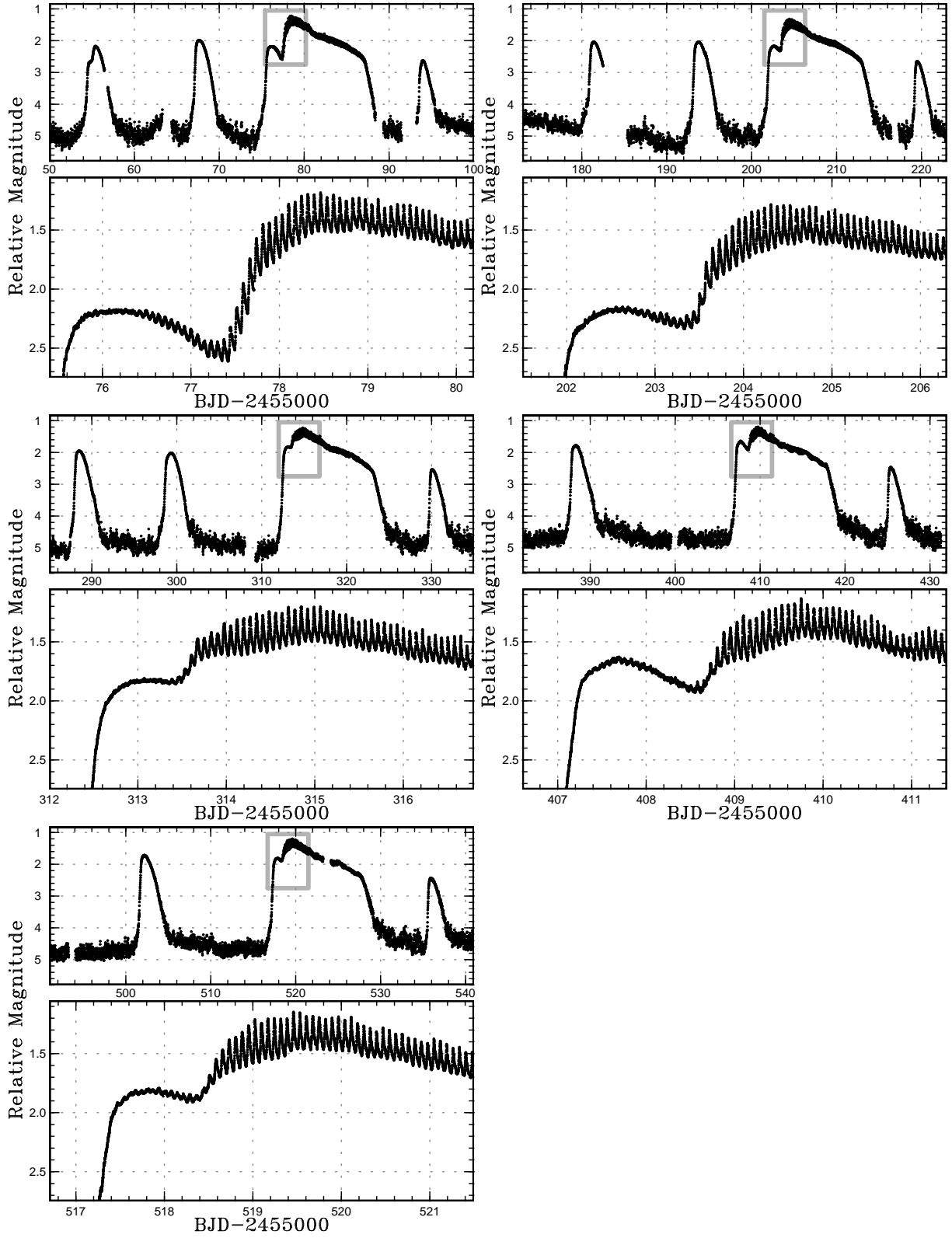


Fig. 4. Enlarged light curves of the five superoutbursts of V1504 Cyg around their start. The Kepler data were averaged to 0.01 d and 0.0005 d bins in the global and enlarged figures, respectively.

secondary remains constant. If all normal outbursts in a supercycle are of the outside-in type, the normal outburst cycle is then lengthened accordingly because the recurrence time of normal outburst is essentially determined by mass supply rate at the disk's outer edge in the case of outside-in outburst. This explains why the number of normal outbursts in a given supercycle is small in Type L supercycle. We note here that the above discussion is based on an assumption of outside-in type outburst. If mass is supplied into the inner part of the disk via a tilted disk, a probability of occurrence of inside-out outburst will be increased. Therefore we must be careful to know whether an outburst is outside-in or inside-out.

Thus the distinction between Type L and S supercycles in V1504 Cyg is now understood as the difference whether the negative superhump exists or not, that is, Type L supercycle is the one accompanied with negative superhumps and Type S is that without them. However, we should note that there are intermediate types of supercycle between these two extreme cases. For instance, in our supercycle No. 6, in which our Kepler data is incomplete, a signal of negative superhumps is visible in its early phase (for a period of about 70 d from BJD 2455530 to BJD 2455600) during which frequent occurrence of normal outbursts is suppressed but it recovered after that as the signal of negative superhumps tapered away around BJD 2455600.

Although we understand a general picture concerning about negative superhumps and occurrence of normal outbursts, a big problem remains to be solved, that is, how the negative superhump (i.e., a tilted disk) is produced in the first place and how it is maintained for a long time. We will discuss the nature of negative superhumps in subsection 3.4 once again.

3.2. *The Start of Superoutburst*

Next we examine how the superoutburst is initiated in V1504 Cyg. It has turned out that all superoutbursts observed in the Kepler data of V1504 Cyg are of precursor-main type. Figure 4 shows enlarged light curves of five superoutbursts of V1504 Cyg in our data and one of such light curves has already been shown in figure 75 of Kato et al. (2012), see also the Kepler light curves shown in Cannizzo et al. (2012). We can see very clearly from figure 4 that periodic humps (which has turned out to be “superhumps” from their period, see power spectrum in figure 3) appear around the maximum of the precursor (that is, a triggering normal outburst) and they continue to grow in amplitude passing local light minimum to the main superoutburst and the time of maximum amplitude of superhumps agree fairly well with that of light maximum of the superoutburst. This is exactly a picture envisioned in the original thermal-tidal model (TTI model) proposed by Osaki (1989).

Although similar phenomena have been observed in other stars before, e.g., V436 Cen (Semeniuk 1980), and QZ Vir (T Leo) (Kato 1997), the Kepler light curve shown here in figure 4 is unprecedentedly clear in this respect. It is quite evident from figure 4 that superhumps are not

a result of superoutburst but rather superhumps (therefore the tidal instability) are most likely the cause of the superoutburst since superhumps start to grow near the precursor maximum. The superhump and superoutburst are so much entwined that one is almost difficult to find any interpretation other than the TTI model, that is, the tidal instability triggers a superoutburst in V1504 Cyg.

Furthermore, Kato et al. (2012) have found transient low-amplitude superhumps in the descending branch of a normal outburst just prior to superoutburst No. 1 (see their figure 78). Similar superhump signatures are also seen in our power spectrum of figure 3 for normal outbursts just prior to superoutbursts No. 2 and No. 3. This phenomenon is very well understood as the failed superhump (or the aborted superhump) discussed by Osaki, Meyer (2003), (see their figure 4).

It is then natural to interpret the periodic humps in the case of VW Hyi discussed by Vogt (1983) as the same sort of phenomenon, (i.e., “failed superhumps”). We believe that the first question concerning about enhanced mass transfer prior of a superoutburst raised by Smak (1996) has been clarified by the Kepler light curve of V1504 Cyg.

As for the second problem raised by Smak (1996), V1504 Cyg shows the precursor-main type superoutburst and the superhump appears in the precursor stage and its amplitude grows with the start of the main superoutburst and it reaches maximum almost with the superoutburst light maximum, that is, the sequence of events observed in V1504 Cyg is exactly as predicted by the original TTI model.

We do not need to address to cases of other SU UMa stars in which no precursor is observed and in which superhumps appear in one or two days after superoutburst maximum. These superoutbursts are understood in the TTI model as follows: in such a superoutburst the disk expands to reach the tidal truncation radius, passing the 3:1 resonance radius during a triggering normal outburst and the viscous plateau stage begins first and then superhumps grow later, as discussed in Osaki, Meyer (2003) and in Osaki (2005) where such a superoutburst is called “Type B” superoutburst. These superoutbursts are expected to occur in low mass-transfer SU UMa systems, which are more numerous in number as compared with high mass-transfer systems such as V1504 Cyg and V344 Lyr.

Let us now turn our attention to the pure thermal instability model advocated by Cannizzo and his group. Cannizzo et al. (2010) made numerical simulations of light curves based on the pure thermal-viscous limit cycle instability and compared their results to the Kepler light curve of V344 Lyr. The Kepler light curves of V344 Lyr also show precursors in superoutbursts which these authors called “shoulders”. These authors succeeded in reproducing shoulder-like structure in their superoutburst light curve but the duration of the shoulder in their simulations was found to be too long compared with those of V344 Lyr. Our criticism to their pure thermal instability model for their explanation of the precursor is not on this point but rather on the following point.

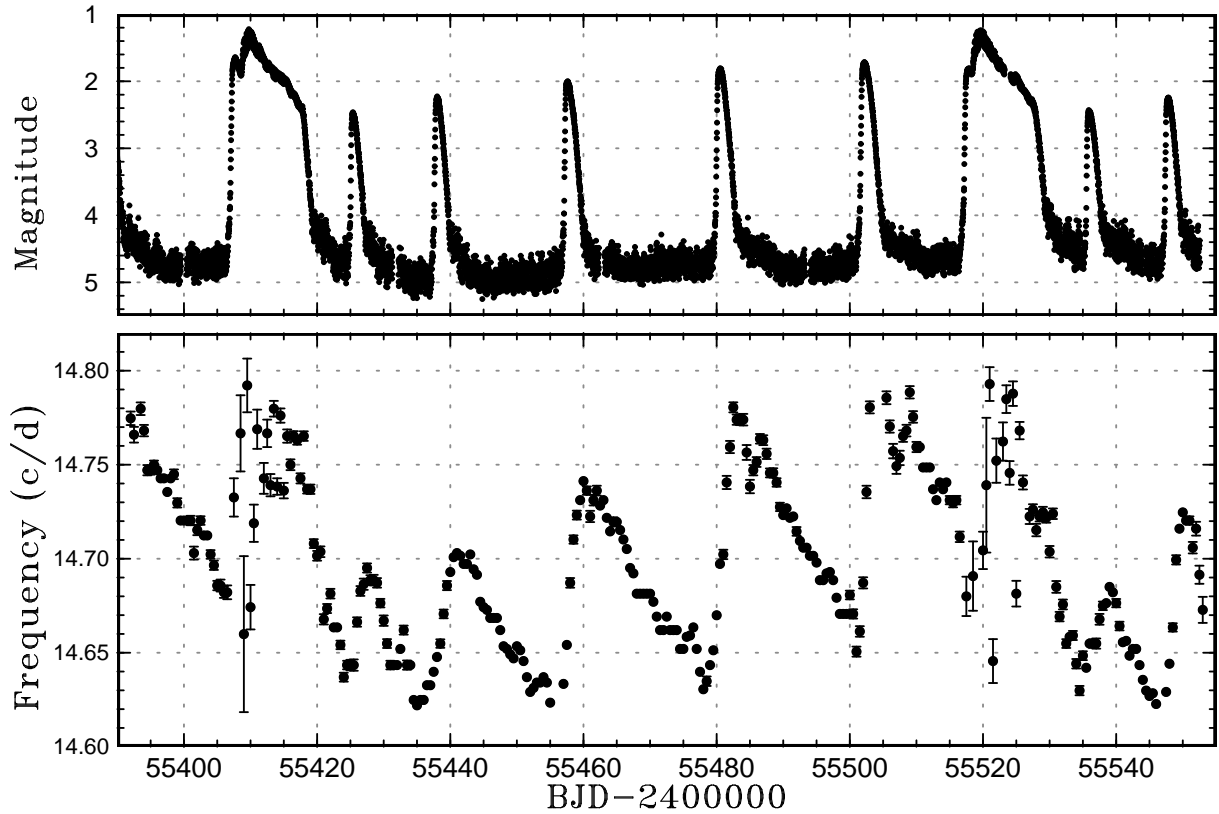


Fig. 5. Time evolution of frequency of the negative superhump covering a complete supercycle No. 5 from BJD 2455390 to 2455550. The upper panel shows light curve while the lower panel does variation in negative superhump frequency in units of cycle per day. The Kepler data were averaged to 0.0005 d bins and the error bars in the lower panel represent $1\text{-}\sigma$ errors in the periods.

In Cannizzo et al. (2010) simulations, a precursor or “shoulder” is produced when the thermal instability starts in the inner part of the accretion disk and the heating front propagates outward but stagnates in the middle of disk for a little while. The heating front restarts to propagate outward to reach the outer edge of the disk which lies at the tidal truncation radius. The long superoutburst ensues. The shoulder is produced when the heating front stagnates in the middle of accretion disk in this model. However, the heating front which stagnates should be never reflected back as a cooling front to produce a superoutburst in their model. This is because the very outburst would have become merely a short normal outburst if it had been reflected. That is, in order to have a long superoutburst in their model, the heating front has to propagate all the way to the outer edge of disk, never being reflected.

Kepler light curves are optical light curves but it is known that the dip between the precursor and main becomes deeper in observations of shorter wavelength, e.g., in the Voyager far-ultraviolet observations of VW Hyi (Pringle et al. 1987), and in EUV observations of OY Car (Mauche, Raymond 2000). In shorter wavelength, the precursor looks like a separate normal outburst. That means that the heating front has to be reflected as a cooling front in the precursor. This observational evidence clearly contradicts with the pure thermal instability model advo-

cated by Cannizzo and his group, because deep dips are never produced in their model.

On the other hand, in the TTI model the precursor is understood as a result of merging of triggering normal outburst with the main body of superoutburst. The degree of merging depends on individual stars and individual superoutbursts, sometimes a precursor is clearly separated from the main superoutburst and looks almost like a normal outburst, sometimes these two merge into one continuation. As discussed in Osaki (2005), in the case of TTI model the heating front is reflected at the outer edge as a cooling front in the triggering normal outburst in the “Type A” superoutburst in which the outer edge of the disk exceeds the 3:1 resonance radius but below the tidal truncation radius. The tidal instability (and thus superhumps) ensues in this triggering normal outburst. As superhumps grow in amplitude, the tidal dissipation is increased in the outer part of the disk and it eventually rekindles hot transition in the outer part of the eccentric disk, which affects most strongly to optical light. A new separate heating front propagates from outer part inward (i.e., a superoutburst is initiated) while the cooling front is still propagating inward. Depending on the relative position of these two fronts, the depths of the precursor dip differ. This explains why the depths of the dip differ in observations of different wavelength and in different stars in TTI model.

As discussed by Schreiber et al. (2004), in order to explain the precursor observed in SU UMa stars, the cooling front has to propagate inward. Cannizzo et al. (2010) model cannot satisfy this requirement and thus the pure thermal instability model is not a viable model for precursor-main type superoutburst in this respect.

3.3. Negative Superhump and Disk Radius Variation

As seen in the power spectrum of figure 3, the negative superhump exists almost always during two supercycles No. 4 and No. 5 and some systematic variation in its frequency is just barely visible in these figures. We have thus made a detailed analysis for the frequency variation of the negative superhump by using the Kepler data for a period from day 380 to day 550 covering a complete supercycle No. 5. Figure 5 illustrates results for the frequency variation of the negative superhump together with light curve of V1504 Cyg. We have calculated its frequency by using a data window of 4 d with time step of 0.5 d. We used phase dispersion minimization (PDM: Stellingwerf 1978) in obtaining the periods and used Fernie (1989) and Kato et al. (2010) for estimating 1- σ errors in the periods. During the superoutburst plateau, we first subtracted the signal of positive superhumps and applied the analysis to the residual signals. Since the amplitudes of negative superhumps were smaller than those of positive superhumps, particularly during around the peaks of superoutbursts, there were relatively large errors in estimating the period of negative superhumps during superoutbursts.

From figure 5 we find a characteristic variation in the negative superhump frequency in a supercycle, reminiscent of the disk radius variation in a supercycle of the TTI model shown in figure 1. In fact, if we accept a tilted disk model for the negative superhump, its frequency has turned out to be a good measure of the disk radius. Furthermore if we use a simplified model for retrograde precession of a rotating Kepler ring of radius R_{eff} , an effective radius representative for the accretion disk, its frequency is given by (see, Larwood 1998)

$$\nu_{\text{NSH}} = \nu_{\text{orb}} \left\{ 1 + \left(\frac{3}{7} \frac{q}{\sqrt{1+q}} \cos\theta \right) \left(\frac{R_{\text{eff}}}{A} \right)^{3/2} \right\}, \quad (1)$$

where ν_{NSH} and ν_{orb} are the frequency for the negative superhump and binary orbital frequency, respectively, $q = M_2/M_1$ is the mass ratio of the binary, R_{eff} the effective disk radius, A is the binary separation, θ is the tilt angle of the disk to the binary orbital plane. We assume $\cos\theta \simeq 1$ for a slightly tilted disk for simplicity. Furthermore if we assume the mass ratio $q = 0.2$ for V1504 Cyg, we can estimate the effective radius, $R_{\text{eff}}/A \simeq 0.34, 0.43, \text{ and } 0.52$ for $\nu_{\text{NSH}} = 14.6, 14.7$ and 14.8 c/d, respectively from equation (1).

We see in figure 5 that the effective disk radius, R_{eff} , shows a saw-tooth pattern with an expansion of the disk in each normal outburst accompanied with contraction during quiescence and the average radius of the saw-tooth pattern increases with advance of supercycle phase. Finally the last normal outburst (which corresponds to a triggering outburst, i.e., a precursor stage of superout-

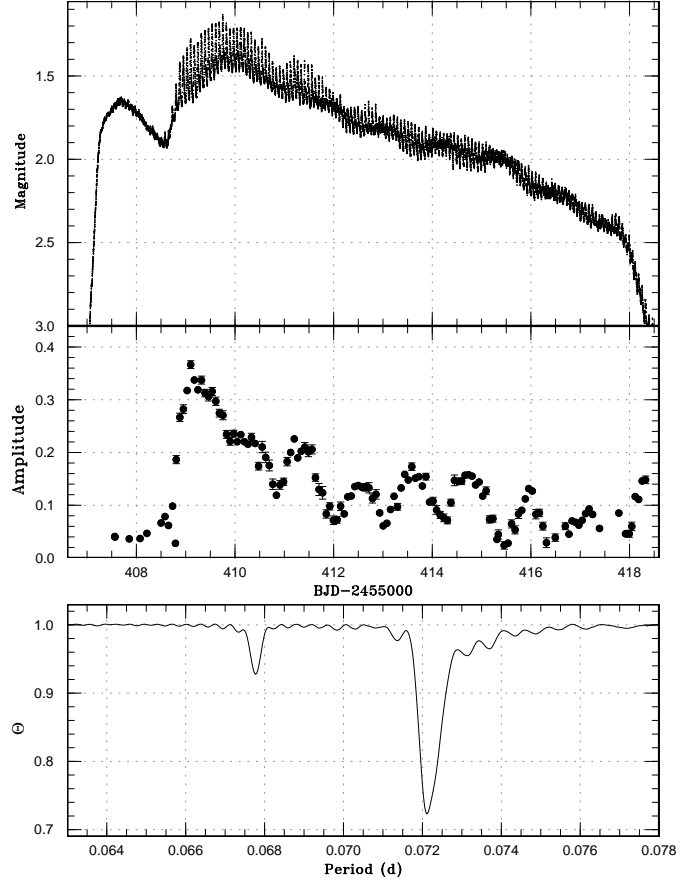


Fig. 6. (Upper:) A light curve of the superoutburst No. 4 showing beating phenomenon between the positive superhump wave and the negative superhump one. The Kepler data were averaged to 0.0005 d bins. (Middle:) Amplitudes of positive superhumps. The amplitudes were determined with the method in Kato et al. (2009). (Lower:) PDM analysis. Both positive and negative superhumps were present.

burst) finally brings the disk to a critical radius, (i.e., the tidal 3:1 resonance instability radius $R_{3:1}/A \sim 0.47$). A superoutburst ensues and a large amount of mass is drained from the disk during a superoutburst and, after the end of the superoutburst, the effective disk radius returns back to a small value, a picture exactly predicted by the TTI model as shown in figure 1. Although the disk radius, R_d , shown in figure 1 and the effective radius, R_{eff} , used here are slightly different, figure 5 exhibits clearly how the angular momentum is accumulated in the disk during a supercycle. The most important prediction of the TTI model concerns about the disk radius variation in a supercycle but its observational test had been difficult before Kepler observations. The Kepler data of V1504 Cyg with the negative superhump now opens a new way to test this prediction.

3.4. Co-existence of Positive and Negative Superhumps

As seen in the two-dimensional power spectra of figure 2 and figure 3, the positive and negative superhumps can

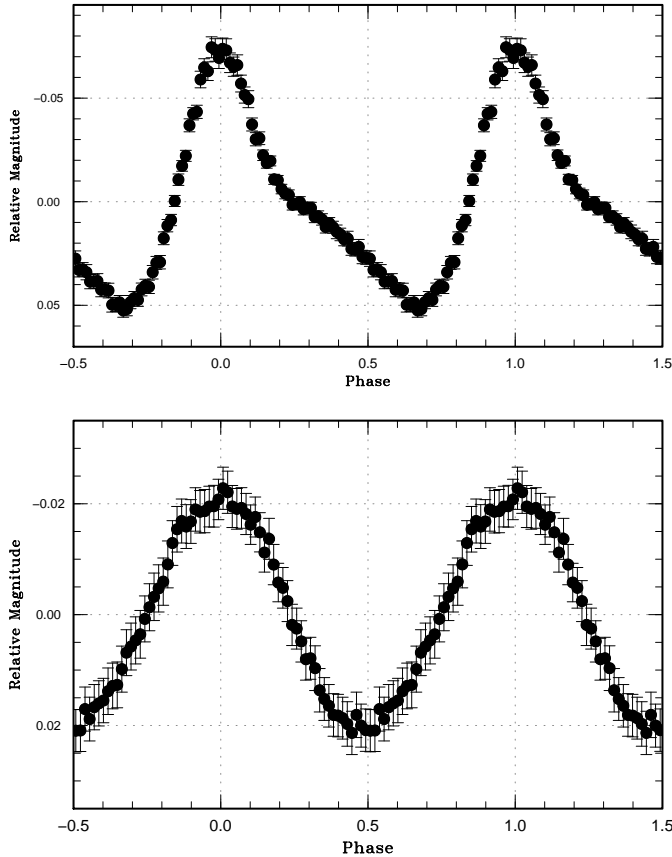


Fig. 7. Phase-averaged light curves of the positive superhump (upper), and of the negative superhump (lower) for the superoutburst No. 4. The periods used for the folding are 0.072183 d and 0.067764 d, respectively.

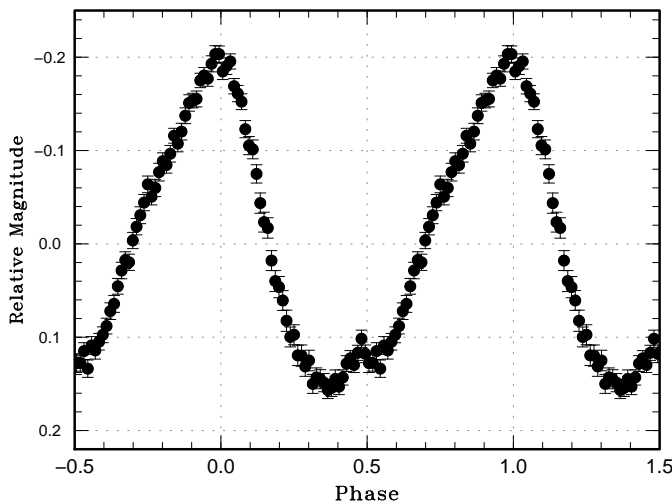


Fig. 8. Phase-averaged light curve of the negative superhump with a period 0.068076 d during quiescence for 8 d of BJD 2455440–448 in V1504 Cyg.

co-exist during a superoutburst, such as the superoutburst No. 4 and No. 5. Figure 6 illustrates a light curve of the superoutburst No. 4 which clearly shows a beating phenomenon of the positive and negative superhumps. The lowest panel of figure 6 shows a PDM diagram in this superoutburst in which two signals at periods 0.067764(10) d (the negative superhump) and 0.072183(4) d (the positive superhump) are visible. The beat period of these two waves is estimated to be about 1.1 d and the amplitude variations with this beat period are seen in the middle panel of figure 6.

This means that the disk in V1504 Cyg develops tilted and eccentric form simultaneously. Figure 7 shows phase-averaged light curves of the positive superhumps (upper panel) and of the negative superhumps (lower panel) for this superoutburst.

The light curve of the positive superhump shown in figure 7 is a typical one for the ordinary superhump seen during a superoutburst, that is, a rapid rise to maximum and slow decline sometimes accompanied with a secondary maximum. On the other hand, the light curve of the negative superhump shows more or less a sinusoidal waveform. For comparison, we show a phase-averaged light curve of the negative superhump in quiescence with a period 0.068076 d during 8 d of BJD 2455440–448 in figure 8. Wood et al. (2011) discussed the Kepler light curve of the negative superhump in quiescence for V344 Lyr, showing that it is approximately saw-toothed with a rise time roughly twice the fall time. Figure 8 shows the same wave pattern as that of V344 Lyr. As discussed by Wood et al. (2011) and mentioned already in subsection 3.1, the quiescence light curve of the negative superhump is understood in terms of gas stream hitting the different part of the disk. We discuss on a possible origin of sinusoidal waveform of the negative superhump during the superoutburst in Appendix.

Amplitudes (in flux) of negative superhumps in the superoutburst No. 4 and in neighboring quiescence are not so much different as seen from figures 2 and 3. In fact, the full amplitudes are 0.04 mag and 0.35 mag, respectively, as seen in figure 7 and figure 8. Since the magnitude difference between the superoutburst and quiescence is about 3 mag in V1504 Cyg, they are similar in flux units. This suggests that mass-transfer rate is not particularly enhanced during the superoutburst. This supports the TTI model rather than the EMT model.

4. Summary

(1) The long outburst of the almost all of dwarf novae below the period gap is accompanied by superhumps. No dwarf novae showing a superoutburst and a well-defined supercycle, but not accompanied with superhumps, have been discovered yet. Since the superoutburst and superhumps are so much entwined as demonstrated in figure 4, any models without taking into account the tidal instability properly do not seem to be correct and we believe that the TTI model is only a viable model for the superoutburst and superhumps of SU UMa stars.

(2) The periodic humps observed in decline phase of a normal outburst just prior to the next superoutburst are found to be of superhump nature and orbital humps are not particularly enhanced in this phase in V1504 Cyg. We conclude no enhancement of mass transfer from the secondary star in this phase and during the start of superoutburst.

(3) The quiescence intervals between normal outbursts are strongly influenced whether negative superhumps exist or not. We confirm conclusion of Ohshima et al. (2012) for ER UMa in that existence of negative superhumps tends to suppress a frequent occurrence of normal outbursts. Two types of supercycles are recognized in V1504 Cyg which are very similar to the Type L and Type S supercycles introduced by Smak (1985) for the case of VW Hyi. Type L supercycle is a supercycle in which the number of normal outbursts is small, typically 5 to 6 while in Type S supercycle it is twice as large (typically around 10) as that of Type L in V1504 Cyg. Type L supercycle is that accompanied with the negative superhump while Type S is that without the negative superhump.

(4) Most of normal outbursts observed in V1504 Cyg are of outside-in type. If so, the increase in quiescence intervals when negative superoutburst appears is understood as due to a decrease in mass supply *at the outer edge* of the tilted disk as gas stream flows over the edge and reaches its inner part in such a case.

(5) The frequency of the negative superhump varies systematically during a supercycle. If we adopt a tilted disk model for the origin of the negative superhump, its frequency represents retrograde precession rate of the tilted disk. Using this variation as an indicator of the disk radius variation, we found that the observed disk radius variation in V1504 Cyg fits very well with a prediction of the TTI model.

(6) The positive superhumps and negative superhumps can co-exist, seen as a beat phenomenon of these two waves in the light curve of the superoutburst No. 4 in V1504 Cyg. This means that the disk can take eccentric and tilted form simultaneously. The amplitude of negative superhump during the superoutburst is not particularly enhanced in flux units as compared with that of neighboring quiescence. This suggests no enhancement of mass-transfer rate during the superoutburst, which supports the TTI model rather than the EMT model for the origin of the superoutburst.

(7) We summarize major consequences about the three models discussed in this paper in the lower part of table 1.

Acknowledgement: We are grateful to Dr. Makoto Uemura for his help in retrieving the Kepler data. One of authors (Y. Osaki) thanks the organizers of a conference held in Warsaw, 2012 September “Accretion Flow instabilities: – 30 years of thermal-viscous instability” for encouraging him to participate, of which experience stimulated him to come back to research in astronomy from his retirement after 7 years of absence. He also would like to express his sincere thanks to Dr. Friedrich Meyer at

Max-Planck-Institut für Astrophysik for encouraging him to write this paper and Professor Hiromoto Shibahashi for enlightening discussions about power spectra. This work was partly supported (TK) by the Grant-in-Aid for the Global COE Program “The Next Generation of Physics, Spun from Universality and Emergence” from the Ministry of Education, Culture, Sports, Science and Technology (MEXT) of Japan. We thank the Kepler Mission team and the data calibration engineers for making Kepler data available to the public.

Appendix 1. Waveform of negative superhump during a superoutburst

The different form of the light curve of the negative superhump during a superoutburst from that of quiescence may suggest that the origin of its light variation is different between superoutburst and quiescence. Let us now discuss the origin of light variation of the negative superhump during a superoutburst. During superoutbursts the disk component will play an important role besides that of gas stream in light variation of negative superhump. Then a question arises why its waveform is sinusoidal if the disk component contributes.

Here we propose a following explanation. Let us consider an eigenmode of oscillation of an accretion disk in which the unperturbed state is co-planar with the binary orbital plane. Here we use the cylindrical coordinates with (r, φ, z, t) in the inertial frame of reference where the center of the coordinates is chosen to be the center of the disk, i.e., the central white dwarf, the azimuthal angle φ is measured in the direction of the binary orbital motion, and the z -axis is that of the binary orbital plane. An eigenmode displacement vector is then written as

$$\xi(r, \varphi, z, t) = (\xi_h, \xi_z) \cos(m\varphi - \omega t), \quad (\text{A1})$$

where ξ is a displacement vector, ω is an eigenfrequency, m is azimuthal wave number, and ξ_h, ξ_z are horizontal and vertical displacements and this mode is denoted as a mode (m, ω) with azimuthal wave number m and eigenfrequency ω .

We do not discuss on the excitation mechanism of tilted disk but we assume here that the disk is tilted with a finite tilt angle θ where $\theta \ll 1$, for simplicity. A tilt of disk is understood to be one of eigenmodes with $m = 1$ and $|\xi_h| \ll |\xi_z|$, $\xi_z \simeq \theta r$ and an eigenfrequency given by angular frequency of retrograde precession $\omega = \Omega_{\text{pr}} < 0$. This mode itself does not produce any light variation. In order to understand light variation of tilted disk, we need to consider an interaction of this mode with the tidal field of the secondary star. The tidal perturbing potential in the accretion disk by the secondary star is expressed by

$$\phi(r, \varphi, z, t) = \phi_m(r, z) \cos(m(\varphi - \Omega_{\text{orb}} t)), \quad (\text{A2})$$

where Ω_{orb} is the angular frequency of the binary orbital motion and $m = 1, 2, 3, \dots$ is azimuthal wave number. The tidal perturbation potential produces deformation in the accretion disk which is described by (see, Lubow 1991, Lubow 1992, Kato 2012)

$$\xi_D(r, \varphi, z, t) = \xi_{D,m}(r, z) \cos(m(\varphi - \Omega_{\text{orb}}t)), \quad (\text{A3})$$

where suffix D denotes deformation.

The wave-wave interaction of the tilt mode with the tidal deformation mode produces $(m-1, m\Omega_{\text{orb}} - \Omega_{\text{pr}})$ mode. In this interaction, the most important one is that of $m=1$, that is, a mode with $(0, \Omega_{\text{orb}} - \Omega_{\text{pr}})$. This mode is independent of the azimuthal angle φ and the time dependence of $\sin\{(\Omega_{\text{orb}} - \Omega_{\text{pr}})t + \delta_0\}$, where δ_0 is a constant phase. That is, this mode produces a sinusoidal time variation with the negative superhump period $P_{\text{NSH}} = 2\pi/(\Omega_{\text{orb}} - \Omega_{\text{pr}})$ where $\Omega_{\text{pr}} < 0$ is retrograde nodal precession rate of a tilted disk. This can produce light variation even with the pole-on geometry, i.e., in the case of inclination angle $i=0$. Light variation with the negative superhump period observed during a superoutburst in V1504 Cyg can be explained by this disk component produced by wave-wave interaction between a tilt mode and the tidal deformation with $m=1$ besides the gas stream component.

References

- Buat-Ménard, V., & Hameury, J.-M. 2002, *A&A*, 386, 891
 Cannizzo, J. K. 1993, in *Accretion Disks In Compact Stellar Systems*, ed. C. Wheeler (Singapore: World Scientific), p. 6
 Cannizzo, J. K., Smale, A. P., Wood, M. A., Still, M. D., & Howell, S. B. 2012, *ApJ*, 747, 117
 Cannizzo, J. K., Still, M. D., Howell, S. B., Wood, M. A., & Smale, A. P. 2010, *ApJ*, 725, 1393
 Cleveland, W. S. 1979, *J. Amer. Statist. Assoc.*, 74, 829
 Fernie, J. D. 1989, *PASP*, 101, 225
 Harvey, D., Skillman, D. R., Patterson, J., & Ringwald, F. A. 1995, *PASP*, 107, 551
 Hellier, C. 2001a, *Cataclysmic Variable Stars: how and why they vary* (Berlin: Springer-Verlag)
 Hellier, C. 2001b, *PASP*, 113, 469
 Hirose, M., & Osaki, Y. 1990, *PASJ*, 42, 135
 Ichikawa, S., Hirose, M., & Osaki, Y. 1993, *PASJ*, 45, 243
 Kato, S. 2012, *PASJ*, submitted
 Kato, T. 1997, *PASJ*, 49, 583
 Kato, T., et al. 2013, *PASJ*, in press (arXiv astro-ph/1210.0678)
 Kato, T., et al. 2009, *PASJ*, 61, S395
 Kato, T., Ishioka, R., & Uemura, M. 2002, *PASJ*, 54, 1029
 Kato, T., et al. 2012, *PASJ*, 64, 21
 Kato, T., et al. 2010, *PASJ*, 62, 1525
 Koch, D. G., et al. 2010, *ApJL*, 713, L79
 Larwood, J. 1998, *MNRAS*, 299, L32
 Lasota, J.-P. 2001, *New Astron. Rev.*, 45, 449
 Lubow, S. H. 1991, *ApJ*, 381, 259
 Lubow, S. H. 1992, *ApJ*, 401, 317
 Mauche, C. W., & Raymond, J. C. 2000, *ApJ*, 541, 924
 Montgomery, M. M., & Martin, E. L. 2010, *ApJ*, 722, 989
 Murray, J. R. 1998, *MNRAS*, 297, 323
 Ohshima, T., et al. 2012, *PASJ*, 64, L3
 Osaki, Y. 1985, *A&A*, 144, 369
 Osaki, Y. 1989, *PASJ*, 41, 1005
 Osaki, Y. 1996, *PASP*, 108, 39
 Osaki, Y. 2005, *Proceeding of the Japan Academy, Series B*, 81, 291
 Osaki, Y., & Meyer, F. 2003, *A&A*, 401, 325
 Pringle, J. E., et al. 1987, *MNRAS*, 225, 73
 Schreiber, M. R., Hameury, J.-M., & Lasota, J.-P. 2004, *A&A*, 427, 621
 Semeniuk, I. 1980, *A&AS*, 39, 29
 Smak, J. 1984, *Acta Astron.*, 34, 161
 Smak, J. 1985, *Acta Astron.*, 35, 357
 Smak, J. 1996, in *IAU Colloq. 158, Cataclysmic Variables and Related Objects*, ed. A. Evans, & J. H. Wood (Dordrecht: Kluwer Academic Publishers), p. 45
 Smak, J. 2000, *New Astron. Rev.*, 44, 171
 Smak, J. 2004, *Acta Astron.*, 54, 221
 Smak, J. 2008, *Acta Astron.*, 58, 55
 Smak, J. 2009, *Acta Astron.*, 59, 121
 Smak, J. I. 1991, *Acta Astron.*, 41, 269
 Smith, A. J., Haswell, C. A., Murray, J. R., Truss, M. R., & Foulkes, S. B. 2007, *MNRAS*, 378, 785
 Stellingwerf, R. F. 1978, *ApJ*, 224, 953
 Still, M., Howell, S. B., Wood, M. A., Cannizzo, J. K., & Smale, A. P. 2010, *ApJL*, 717, L113
 Truss, M. R., Murray, J. R., & Wynn, G. A. 2001, *MNRAS*, 324, 1P
 van Paradijs, J. 1983, *A&A*, 125, L16
 Vogt, N. 1983, *A&A*, 118, 95
 Warner, B. 1995, *Cataclysmic Variable Stars* (Cambridge: Cambridge University Press)
 Whitehurst, R. 1988, *MNRAS*, 232, 35
 Wood, M. A., Still, M. D., Howell, S. B., Cannizzo, J. K., & Smale, A. P. 2011, *ApJ*, 741, 105